Electronic Supplementary Information

1.1. Materials and equipment

The buffer components were purchased from Sigma-Aldrich (USA) or Lach-Ner (Czech Republic). ScintiSafe 3 (Fisher Scientific, USA) scintillation cocktail was used for counting the samples. Whatman GF/B (Aldrich, USA) filters were used for the filtration assays. Radioactivity of samples was measured using a Wallac 1219 Rackbeta (LKB Instruments, USA) liquid scintillation counter. The purity of ligands was determined by high-performance liquid chromatography (HPLC; Agilent 1260–1290; USA) analysis, at wavelengths of 220 and 254 nm. The purity was at least 95% at both wavelengths. Nuclear magnetic resonance (NMR) spectra were measured using a Bruker Avance-III (Germany) 700 MHz spectrometer. High-resolution mass spectra (HRMS) were obtained using Varian 910-FT-ICR (USA) mass spectrometer.

1.2. Ligand synthesis

PE2I precursor was radiolabelled with [^{3}H]MeI as described previously.[1] [^{3}H]PE2I is a tritium labelled version of PE2I, where the hydrogens of methyl ester group have been replaced with tritium. [^{3}H]PE2I had a specific radioactivity of 69.4 Ci/mmol. PE2I and 2α-PE2I were synthesised, starting from cocaine hydrochloride, in a similar way as described before.[2] After step (iii), the 2α-derivative (upper structure) and 2β-derivative (lower structure) were isolated and the synthesis was continued separately (Scheme S1). The products of synthesis were characterised by ^{1}H, ^{13}C NMR and HRMS. The stereoconfiguration was determined by NMR.

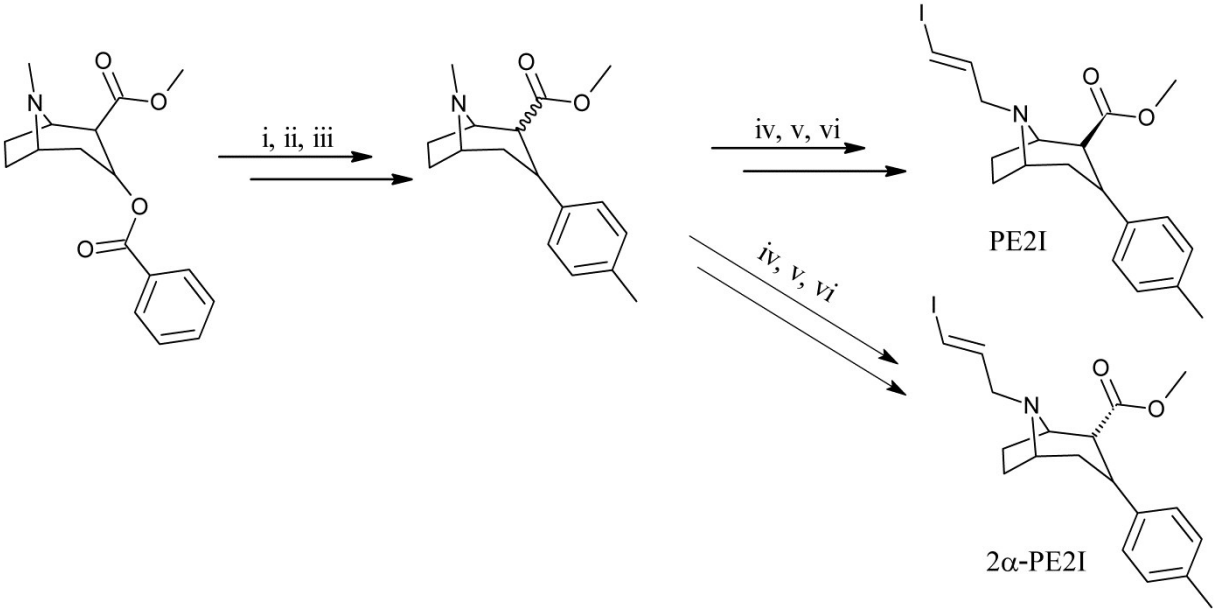

Scheme S1 (i) HCl, 120 °C, 24 h; (ii) (a) POCl, 120 °C, 4–5h, (b) MeOH, −45 °C, 15 min, rt. 12 h; (iii) (a) p-tolylmagnesium bromide, Et_2O, CH_2Cl_2, −40–50 °C, 2–4h, (b) TFA, −80 °C; (iv) (a) 2,2,2-trichloroethyl chloroformate, 120–130 °C, 2 h, (b) Zn, AcOH, rt. overnight; (v) 1-chloro-3-tributylstannyl-prop-2*E*-ene, EtOH, TEA, KI, 90 °C, 16 h; (vi) I_2, $CHCl_3$, 0 °C, 2–3h.

PE2I

^{1}H NMR ($CDCl_3$ + TMS, 700 MHz): δ 1.63–1.68 (m, 2H), 1.75 (ddd, 1H, *J*=4.5, 9.3, 13.1), 1.94–1.99 (m, 1H), 2.03–2.09 (m, 1H), 2.29 (s, 3H), 2.60 (dt, 1H, *J*=2.7, 12.6 Hz), 2.82 (ddd, 1H, *J*=0.9, 6.7, 14.7 Hz), 2.90 (t, 1H, *J*=4.0 Hz), 2.94 (ddd, 1H, *J*=1.7, 5.2, 14.4 Hz), 2.99 (td, 1H, *J*=5.0, 12.9 Hz), 3.39 (m, 1H), 3.53 (s, 3H), 3.64 (m, 1H), 6.20 (d, 1H, *J*=14.4 Hz), 6.49 (ddd, 1H, *J*=5.2, 7.1, 14.3 Hz), 7.08 (d, 2H, *J*=8.0 Hz), 7.15 (d, 2H, *J*=8.0 Hz).

^{13}C NMR ($CDCl_3$ + TMS, 176 MHz): δ 21.0, 25.8, 26.1, 33.8, 34.1, 51.1, 52.7, 58.0, 61.4, 62.4, 127.2, 128.7, 135.3, 139.8, 144.4, 171.8.

2α-PE2I

^{1}H NMR ($CDCl_3$ + TMS, 700 MHz): δ 1.59–1.63 (m, 1H), 1.69–1.73 (m, 1H), 1.78–1.82 (m, 2H), 1.95–2.00 (m, 2H), 2.28 (s, 3H), 3.03 (dd, 1H, *J*=1.8, 11.9 Hz), 3.05–3.12 (br, 3H), 3.28 (br, 1H), 3.42 (m, 1H), 3.48 (s, 3H), 6.29 (d, 1H, *J*=14.4 Hz), 6.63 (td, 1H, *J*=6.3, 14.4 Hz), 7.06 (d, 2H, *J*=7.9 Hz), 7.12 (d, 2H, *J*=8.0 Hz).

^{13}C NMR ($CDCl_3$ + TMS, 176 MHz): δ 21.0, 23.4, 26.5, 36.6, 38.9, 51.38, 51.43, 56.4, 59.1, 61.7, 77.7, 127.5, 129.1, 135.8, 140.5, 143.8, 173.3.

Compound	Molecular formula	Molecular ion formula	Exact m/z $[M+H]^+$	Measured m/z, $[M+H]^+$	Error, ppm
PE2I	$C_{19}H_{24}O_2NI$	$C_{19}H_{25}O_2NI^{+1}$	426.09245	426.09204	**-0.96**
2α-PE2I	$C_{19}H_{24}O_2NI$	$C_{19}H_{25}O_2NI^{+1}$	426.09245	426.09212	**-0.77**

Table S1 Results of HRMS analysis of PE2I and 2α-PE2I

1.3. Membrane preparation

Membrane fragments of striata from adult C57BL/6 mice (mDAT) were used in experiments with the radioligand. The striata were rapidly dissected, frozen and stored at −80 °C. The tissue was suspended in approximately 0.3 ml of ice-cold buffer (120 mM NaCl, 30 mM HEPES, 5 mM KCl, pH 7.4) per mg of wet tissue, sonicated with an ultrasound homogeniser (Bandelin SONOPULS; 3 × 15 sec), and centrifuged at 30,000 × *g* at 0 °C for 15 min. The supernatant was discarded and the remaining pellet was resuspended in buffer and homogenised again. This procedure was repeated three more times to yield a final membrane suspension that was divided into aliquots and stored at −80 °C until needed. The final membrane concentration was approximately 4 mg of wet tissue/ml.

1.4. Kinetic experiments

1,000 µl of membrane suspension was transferred to a thermostated cuvette at 25 °C and 500 µl of [^{3}H]PE2I (final concentration, 3 nM) and unlabelled ligand (final concentration, 1…30 nM) solution was added. If the effect of [^{3}H]PE2I concentration to k_{obs} was studied, 500 µl of [^{3}H]PE2I (final concentration, 1…30 nM) was added to 1,000 µl of membrane suspension. Aliquots were taken at predetermined time intervals, filtered through GF/B filters (pre-soaked in 0.3% polyethylene imine solution) and washed with 5 ml of ice-cold buffer (20 mM

potassium phosphate, 100 mM NaCl, pH 7.4), air-dried, and transferred to scintillation vials; 5 ml of scintillation cocktail was then added. The vials were then shaken approximately 12 h before the radioactivity was measured using a liquid scintillation counter. Specific binding was calculated as the difference between the total binding and the nonspecific binding. Data were analysed with GraphPad Prism 4 (USA) software package.

Data from the kinetics experiments, which were performed under pseudo-first order conditions, followed the exponential rate equation (Eq. S1):

$$B_t = B_{ns} + B_{eq}\left(1 - exp^{-k_{obs}t}\right) \qquad \text{Eq. S1}$$

where B_t is the total binding at time t, k_{obs} is the observed rate constant, and B_{ns} and B_{eq} are the nonspecific and specific binding at equilibrium, respectively.[3]

1.5. Two-step radioligand binding mechanism

Radioligand [^{3}H]PE2I is known to bind with dopamine transporter (DAT) in a two-step mechanism[4] in which the fast binding step is followed by a slow step of the complex isomerisation (Scheme S2):

$$\mathbf{R + L^*} \underset{}{\overset{K^*_{L^*}}{\rightleftharpoons}} \mathbf{RL^*} \underset{k^*_{-i}}{\overset{k^*_i}{\rightleftharpoons}} \mathbf{(RL^*)}$$

Scheme S2

where K^*_{L*} is the equilibrium dissociation constant for the DAT-ligand complex RL*, and k^*_i and k^*_{-i} denote the rate constants of the complex isomerisation and de-isomerisation processes, respectively. The presence of the slow isomerisation step is the reason for the slow observed off-rate of the ligand from the DAT binding site; i.e. the residence time is long.

The kinetic parameters of Scheme S2 can be calculated from the k_{obs} vs. ligand concentration plot (Eq. S2):

$$k_{obs} = \frac{k^*_i[L^*]}{K^*_{L^*} + [L^*]} + k^*_{-i} \qquad \text{Eq. S2}$$

where L* is radioligand and R stands for the receptor; i.e. DAT in this study.[3] The kinetic analysis performed for [^{3}H]PE2I interaction with the DAT binding sites yielded the following parameters, which are in agreement with previous data:[4]

$K^*_{L*} = 26 \pm 12$ nM
$k^*_i = 0.024 \pm 0.005$ s^{-1}
$k^*_{-i} = 0.0022 \pm 0.0008$ s^{-1}

1.6. Influence of unlabelled ligands on radioligand binding kinetics with DAT

The mechanism of binding of unlabelled ligand L with DAT can be analysed by studying its influence on the kinetics of the [^{3}H]PE2I interaction with DAT sites. For this analysis, the time course of radioligand L* binding with the DAT sites should be monitored in the presence of different L concentrations, and the two following kinetic mechanisms can be differentiated.

In the first case, if the unlabelled ligand L is able to initialise the complex RL isomerisation, the overall process of radioligand L* binding with binding sites R is described by Scheme S3:

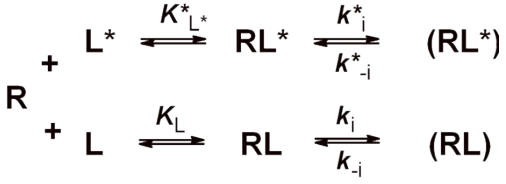

Scheme S3

where the kinetic parameters $K^*_{L^*}$, k^*_i and k^*_{-i} characterise the radioligand L* interaction with DAT sites and parameters K_L, k_i and k_{-i} characterise the interaction of the unlabelled ligand with the same binding sites.

As both ligands L* and L consume the same binding sites of the same pool of sites for forming complexes (RL*) and (RL), the observed rate of decrease of R depends on both reactions, and the rate constant k_{obs} for the overall process decreases. This situation is described by the following rate equation (Eq. S3):

$$k_{obs} = \frac{k^*_i[L^*]}{K^*_{L^*} + [L^*]} + \frac{k_i[L]}{K_L + [L]} + \frac{k^*_{-i} + k_{-i}}{2} \qquad \text{Eq. S3}$$

where parameters $K^*_{L^*}$, k^*_i and k^*_{-i} and K_{L^*}, k_i and k_{-i} correspond to the reaction scheme S4. Detailed derivation of Eq. S5 has been published previously [5,6]. The positive slope of the k_{obs} vs. [L] plot, measured at a constant radioligand concentration, is the diagnostic tool for the reaction scheme S4. Very importantly, this approach can be used without the need for more sophisticated kinetic analysis.

However, if a more detailed description of the mechanism of the interaction of L with R is needed, the kinetic analysis can easily be extended for determination of the appropriate kinetic parameters, taking into consideration that at constant radioligand L* concentration, the k_{obs} vs. [L] plot simplifies and can be fitted to the following hyperbolic function (Eq. S4)

$$k_{obs} = \frac{k_i[L]}{K_L + [L]} + C \qquad \text{Eq. S4}$$

In this equation, k_{obs} is the observed rate constant of radioligand binding and parameters k_i and K_L characterise the interaction of the non-radioactive ligand L with the DAT binding sites. The parameter C in Eq. S4 summarises the first and last terms of Eq. S3, which remain constant if experiments are conducted at the same radioligand concentration, and can be used

to calculate k_{-i}. This analysis yielded the following kinetic parameters for PE2I interaction with the DAT binding sites:

$K_L = 37 \pm 24$ nM
$k_i = 0.020 \pm 0.008$ s^{-1}
$k_{-i} \approx 0.0024$ s^{-1}

It can be seen that direct kinetic assay of radioligand binding and the kinetic study of the interaction of non-radioactive ligands with the receptor sites by using radioactive reporter ligand gave rather consistent results.

Secondly, if the unlabelled ligand does not initiate isomerisation of the binding protein, competition of L with L* for the same binding site can be observed and described by the following reaction scheme (Scheme 4):

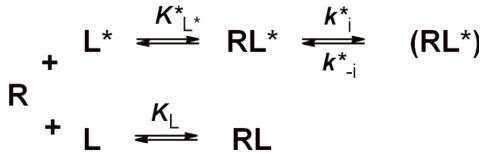

Scheme S4

The observed rate constants k_{obs}, which characterise radioligand L* interaction with the binding sites R in the presence of different concentrations of the unlabelled ligand L, follow a declining hyperbolic dependence (Eq. 5):

$$k_{obs} = \frac{k^*_i [L^*]}{\left(1 + [L]/K_L\right) K^*_{L^*} + [L^*]} + k^*_{-i} \qquad \text{Eq. S5}$$

and the negative slope of this plot, measured at constant radioligand concentration, is the diagnostic tool for the reaction scheme S3. In this rate equation, k_{obs} is the apparent rate constant of radioligand L* binding to DAT, determined at radioligand concentration [L*] in the absence and in the presence of non-radioactive ligand L. Parameters $K^*_{L^*}$, k^*_i and k^*_{-i} characterise radioligand interaction with DAT sites as shown in Eq. S2, and K_L is the equilibrium dissociation constant for the interaction of the unlabelled ligand L with the binding sites R. Processing experimental data according to Eq. S3 yielded a K_L value of 58 ± 23 μM for 2α-PE2I interaction with DAT.

1.6. Long and short residence time diagnostics

Differentiation between ligands, characterised by slow and fast off-rate or by long and short residence times, can be proposed on the basis of the described kinetic analysis. This procedure is based on investigation into the influence of a non-radioactive ligand on the value of the

observed rate constant k_{obs} for radioligand binding, and two different situations can be observed.

First, if the presence of a non-radioactive ligand decreases the k_{obs} values, and the slope of the k_{obs} vs. [L] plot is negative (Fig. 1F), the ligand is characterised by fast off-rate and a short residence time.

Second, if the slope of the k_{obs} vs. [L] plot is positive, the ligand is characterised by slow off-rate and a long residence time.

These two simple guidelines allow qualitative differentiation between slow and fast residence times. It is important to emphasise that L concentration around its IC_{50} value should be used for clear differentiation between these binding mechanisms.

The same kinetic approach allows quantification of residence time if the hyperbolic dependence of k_{obs} vs. [L] can be measured. In this case, Eq. S3 should be used for data processing, taking into consideration all kinetic parameters of the radioligand interaction with the binding site. Quantification of the short residence time cannot be made using this simple procedure and needs facilities for the kinetic study of fast reactions. However, in most cases differentiation between the short and long residential times is sufficient for application of this metric for description of drug–receptor interactions and application of structure–activity or structure–kinetics analysis.

References

1. V. Stepanov, M. Schou, J. Järv and C. Halldin, *Appl. Radiat. Isot.*, 2007, **65**, 293–300.
2. L. Garreau, P. Emond, C. Belzung, D. Guilloteau, Y. Frangin, J.-C. Besnard and S. Chalon, *J. Pharmacol. Exp. Ther.*, 1997, **282**, 467–474.
3. J. Järv, B. Hedlund and T. Bartfai, *J. Biol. Chem.*, 1979, **254**, 5595–5598.
4. V. Stepanov and J. Järv, *Neurosci. Lett.*, 2006, **410**, 218–221.
5. S. D. Varfolomeev and S. V Zaitsev, Moscow State Univ. Moscow, 1982. *In Russian*.
6. M. Eller, J. Järv and P. Palumaa, *Org. React.*, 1988, **25**, 372–386.